

Magnon-polaron and Spin-polaron Signatures in the Specific Heat and Electrical Resistivity of $La_{0.6}Y_{0.1}Ca_{0.3}MnO_3$ in Zero Magnetic Field, and the Effect of $Mn - O - Mn$ Bond Environment

M. Ausloos¹, L. Hubert¹, S. Dorbolo^{1,2}, A. Gilabert³
and R. Cloots⁴

¹ SUPRAS, Institute of Physics, B5,

University of Liège, B-4000 Liège, Euroland

² SUPRAS, Montefiore Electricity Institute, B28,

University of Liège, B-4000 Liège, Belgium

³ Laboratoire de Physique de la Matière Condensée,

Université de Nice-Sophia Antipolis,

Parc Valrose F-09016 Nice, Cedex 02, France

⁴ SUPRAS, Institute of Chemistry, B6,

University of Liège, B-4000 Liège, Belgium

October 29, 2018

Abstract

$La_{0.6}Y_{0.1}Ca_{0.3}MnO_3$, an ABO_3 perovskite manganite oxide, exhibits a non trivial behavior in the vicinity of the sharp peak found in the resistivity ρ as a function of temperature T in zero magnetic field. The various features seen on $d\rho/dT$ are discussed in terms of competing phase transitions. They are related to the $Mn - O - Mn$ bond environment depending on the content of the A crystallographic site. A Ginzburg-Landau type theory is presented for incorporating concurrent phase transitions. The specific heat C of such a compound is also examined from 50 till 200 K. A log-log analysis indicates different regimes. In the low temperature conducting ferromagnetic phase, a collective magnon signature ($C \simeq T^{3/2}$) is found as for what are called magnon-polaron excitations. A $C \simeq T^{2/3}$ law is found at high temperature and discussed in terms of

the fractal dimension of the conducting network of the weakly conducting (so-called insulating) phase and Orbach estimate of the excitation spectral behaviors. The need of considering both independent spin scattering and collective spin scattering is thus emphasized. The report indicates a remarkable agreement for the Fisher-Langer formula, i.e. $C \sim d\rho/dT$ at second order phase transitions. Within the Attfield model, we find an inverse square root relationship between the critical temperature(s) and the total local $Mn - O - Mn$ strain.

1 Introduction

The properties of manganite's family $R_{1-x}A_xMnO_3$ compounds (where $R = La, Y, Nd, Pr$ and $A = Ca, Sr, Ba, Pb$) with a Mn^{3+}/Mn^{4+} mixed valence keep attracting much attention of both experimentalists and theorists. [1, 2, 3, 4, 5, 6, 7, 8, 9, 10, 11, 12, 13, 14, 15, 16, 17, 18, 19, 20, 21, 22, 23, 24, 25, 26, 27] In the doping range $0.2 < x < 0.5$, these compounds are known to undergo a double magnetic and conductive phase transition under cooling from a paramagnetic (PM) weakly conductive, usually called *insulating* (I), state to a ferromagnetic (FM) metallic-like (M) state. Thus a Curie temperature T_C and a charge carrier localization temperature T_{MI} are respectively defined. The observable difference between the two critical temperatures is usually attributed to the quality of the sample [8, 9, 10, 11]. Nevertheless it could be ascribed to intrinsic interaction interplays, enhanced by the inhomogeneity content. No need to recall that some anomalous expansion also takes place at the transitions, [26] thus indicating a strong coupling between the lattice, spin, and electronic degrees of freedom.

The magnetic localization of spin polarized carriers, forming so-called *spin polarons* results in a diffusivity dominated charge carrier transport mechanism below T_C with a steadily increasing resistivity ρ with increasing temperature. However above T_C , the resistivity decreases and follows a thermally activated Mott-like variable-range hopping law $\rho \propto \exp(T_0/T)^z$ with $1/4 \leq z \leq 1$. Despite a variety of theoretical scenarios attempting to describe this phenomenon, practically all of them adopt as a starting point the so-called double-exchange (DE) mechanism, which considers oxygen mediated electron exchange between neighboring Mn^{3+}/Mn^{4+} sites and strong on-site Hund's coupling. In other words, the mobility of the conduction electrons between heterovalent Mn/Mn pairs is supposed to be greatly enhanced when the magnetic moments on adjacent Mn ions are aligned. The mixed valency also leads to the formation of small polarons, arising from Mn/Mn valence changes and Jahn-Teller (JT) distortions involving Mn that leads to incoherent hopping and high resistivity in the insulating phase. The estimated exchange energy [15] $JS = 45meV$ (where $S = 2$ is an effective spin on a Mn site), being much less than the Fermi energy E_F in these materials (typically, $E_F = 0.15eV$), favors an FM ground state.

The localization scenario, [17] in which Mn oxides are modelled as systems with both DE off-diagonal spin disorder and nonmagnetic diagonal disorder,

predicts a divergence of the electronic localization length $\xi(M)$ at some so called M-I phase transition at T_{MI} . A critical spontaneous magnetization M strength separates both phases, i.e. for M small, $0 < M < M_0$, the system is in a highly resistive (insulator-like) state, while at low T, for $M > M_0 > 0$, the system is in a low resistive, metallic-like, ferromagnetic phase. Within this scenario, the Curie point T_C is defined through the spontaneous magnetization M as $M(T_C) = 0$, while the M-I transition temperature T_{MI} is such that $M(T_{MI}) = M_0$ with M_0 being a fraction of the saturated magnetization M_s , thereby with $T_{MI} < T_C$.

The influence of magnetic fluctuations on electron-spin scattering near T_{MI} and T_C is expected to be rather important. They might easily tip a subtle balance between magnetic and electronic processes in favor of either charge localization or delocalization, and shift the relative position of T_{MI} and T_C . Moreover as in any phase transitions, a relevant question pertains to the observation or not of critical fluctuations [22], and the order of the transition. [26] It seems that the ferromagnetic ordering is a thermodynamic first-order transition, intrinsically broadened by a distribution in T_C [26]. We will give an interpretation of that broadening, and its fine structure, from a chemical point of view.

An applied magnetic field H enhances the FM order, thus reduces the spin scattering and produces a negative so-called giant magnetoresistivity (GMR). A sharp peak occurs around T_{MI} . The localized spin disorder scattering is thought to be highly responsible for the observed features in the GMR [17]. We will not report magnetic field effects here below.

In view of its charge carrier density sensitive nature, specific heat measurements complement the traditional ρ and GMR data and be used as a tool for probing the intrinsic delocalization of the charge carriers below T_{MI} , whence below T_C . The observed [18] giant magnetic *entropy change* in manganites (produced by the abrupt reduction of the magnetization and congruent to an anomalous thermal expansion near the Curie point) gives another reason to utilize the specific heat data in order to get an additional information on the underlying interaction mechanisms in these materials as well as on excitations present in the vicinity of the critical temperature(s) [24, 25, 26, 27].

On the other hand, substitution on the A (or R) site is known to modify the phase diagram through cation size effects leading toward either a charge-ordered (CO) or an antiferromagnetic (AFM) instability [9]. In particular, Y substitution is responsible for weakening the system's robustness against strong AFM fluctuations, developed locally within the ordered FM matrix thereby shifting T_C . Some difference in T_C and T_{MI} positions related to modified collective excitations can be expected.

In $La_{0.6}Y_{0.1}Ca_{0.3}MnO_3$, [3] the negative GMR $\Delta\rho$ observed at $B = 1T$ shows a fine symmetry around $T_0 = 160K$. This suggests a usual transport mechanism controlled by fluctuations, in a polycrystalline or inhomogeneous system, since it is known that the transition should be very sharp for single grains [23]. There are indications [14] that the observable GMR $\Delta\rho(T, B)$

scales with the magnetization M in the ferromagnetic state and follows an M^2 dependence in the paramagnetic region implying thus some kind of universality in the magneto-electrical transport properties below and above T_C , as in metals [28, 29, 30, 31, 32, 33]. Strong magnetic (and charge) fluctuations are thought to be triggered by Y substitution and further enhanced by the magnetic field. The [19, 20] data was interpreted in terms of nonthermal spin hopping and magnetization M dependent charge carrier localization leading to $\Delta\rho = -\rho_s \left(1 - e^{-\gamma M^2}\right)$ with $M(T, B) = CB/|T - T_C|^\nu$ [19]. This formula generalizes the usual law for independent spin scattering in metals [28, 29, 30].

In the present paper we report and discuss some analysis of typical results on the specific heat for a $La_{0.6}Y_{0.1}Ca_{0.3}MnO_3$ sample from the same batch previously used to measure the GMR and magneto-thermoelectric power (MTEP) [19, 20]. A wide temperature interval ranging from 20K to 300K has been investigated with great care, using a PPMS from Quantum Design [34] when it works. The method is a semi-adiabatic experiment. We observe contributions from the collective spin reservoir. For the electrical resistivity the same care was taken as in investigations aimed at measuring critical exponents [35, 36].

From the theoretical point of view we adopt the main ideas of the microscopic localization theory [17] and can construct a phenomenological free energy functional of Ginzburg-Landau (GL) type which describes the temperature behavior of the spontaneous magnetization in the presence of strong localization effects. Calculating the background and fluctuation contributions to the total magnetization within the GL theory, the localization related magnetic free energy leads to the specific heat through

$$C = -\frac{\partial^2 \mathcal{F}}{\partial T^2}. \quad (1)$$

It is also known [37] that when (critical) fluctuations are important, the specific heat C and $d\rho/dT$ contain the same temperature dependent kernel, thus

$$C \simeq \frac{\partial \rho}{\partial T}. \quad (2)$$

2 Experimental results

The $La_{0.6}Y_{0.1}Ca_{0.3}MnO_3$ samples were prepared from stoichiometric amounts of La_2O_3 , Y_2O_3 , $CaCO_3$, and MnO_2 powders, among many other cases. The mixture was heated in air at 800°C for 12 hours to achieve decarbonation and was pressed at room temperature under $10^3 kG/cm^2$ in order to obtain parallelepipedic pellets. A slow (during 2 days) annealing and sintering process was made from 1350°C to 800°C in order to preserve the stoichiometry, though no perfect sample homogeneity is claimed.

A small bar (length $l = 10\text{mm}$, cross section $S = 4\text{mm}^2$) was cut from one pellet. The electrical resistivity $\rho(T)$ was measured using the conventional four-probe method, taking a data point every 0.5K. To avoid Joule and Peltier effects, a DC current $I = 1\text{mA}$ was injected (as a one second pulse) successively on both sides of the sample. The voltage drop V across the sample was measured with high accuracy by a $KT182$ nanovoltmeter. Measurements *in a magnetic field* indicated a magnetoresistance (MR) $\Delta\rho(T, H) = \rho(T, H) - \rho(T, 0)$ as shown in Fig. 1 in ref.[19]. The negative MR $\Delta\rho(T, H)$ shows a peak at some temperature *ca.* $T^* = 170$ K. The magneto thermopower (MTEP) S was also measured as reported elsewhere [20].

However further examination of $d\rho/dT$ shows some fine structure, as seen in Fig.1. The inflexion point of ρ is precisely defined through $d\rho/dT$ at $T = 149$ K, the maximum in ρ occurs for $d\rho/dT = 0$ at $T = 170$ K. A second inflexion point occurs at 188 K. Moreover one observes a singularity in $d\rho/dT$ above the inflexion point, i.e. at $T = 158$ K, and λ -like peaks at 94, 110, and 130 K. This may be reminding us of $d\rho/dT$ behavior at ferromagnetic transitions in metals and suggests the existence of specific energies.

We were able in [19] to successfully fit the $\Delta\rho(T, B)$ data, where Δ means the deviation from the $B=0$ case, for the whole temperature interval with

$$\Delta\rho(T, B) = -A[1 - e^{-\beta(T)}], \quad (3)$$

where

$$\beta(T) = \beta_0 \left[\frac{T_0}{T - T_0} \right]^{2\nu}, \quad (4)$$

in which A , β_0 and ν are temperature-independent parameters, under the condition $T_0 = T^*$. Furthermore we observe that the $d\rho/dT$ behavior rather looks like the change in resistivity occurring near most anti- and/or ferromagnetic order-disorder phase transitions [30, 33, 37, 38, 39].

Next, Fig. 2 shows a typical unsmoothed run for the temperature behavior of the specific heat $C(T)$, from which the ratio $C(T)/T$ is obtained (Fig. 1). Practically, a 10 mg sample has been placed on a sample holder composed of a little paddle ($3 \times 3 \text{ mm}^2$) in teflon. A heater placed on the back of the paddle increases the temperature of the sample during 3 s; a data point is taken every 1.5K. Both thermal answers of sample holder and sample are recorded and fitted by exponential laws for which the characteristic time is related to the thermal capacity of the system. The addendum contribution has to be first measured and subtracted from the raw data. We stress that this is done for the same sample as that used for measuring the MR. It is observed that singularities occur at the *same* temperatures for C and $d\rho/dT$. In the intermediate temperature regime hereby examined (from 108 till 156K) the rather flat though quite bumpy behavior reflects the complex phase transition dynamics and complicated contributions from the spin-phonon-electron system.

For a general input at this point, let us recall a few specific heat data, like that on CaMnO_3 characterized by a $T_N = 131$ K [27], or that on $\text{La}_{0.875}\text{Ca}_{0.125}\text{MnO}_3$ which presents *three* well spread anomalies at 315, 146 and 80 K, and a broad (hysteretic) feature at 35K [24].

Finally, it is well known that the specific heat has simple behaviors at low T, arising from different mechanisms :(i) the electronic contribution, i.e. $C_e \simeq T$, (ii) the phonon contribution, as $C_\omega \simeq T^3$, and (iii) the magnon contribution, i.e. $C_{\text{magn}} \simeq T^{3/2}$. [40] Since the data has been very finely taken we can expect to treat it as when searching for critical exponents on a log-log plot. In the temperature interval so examined three regimes are markedly evident, see Fig. 3. At *low* temperature a 3/2 exponent is observed till $T = 94\text{K}$, followed by a linear temperature regime up to $T = 156$ K, thereafter followed by a $T^{2/3}$ regime. Okuda et al. [25] have also recently reported that around the M-I transition T^3 and $T^{1.5}$ components are observed in the specific heat, in a $\text{La}_{1-x}\text{Ca}_x\text{MnO}_3$ series at low temperature (below 10K).

3 Discussion

Since we are mainly dealing with the temperature changes below the transition temperature(s), it is reasonable to assume that the observed behaviors can be attributed to a phonon and an electron background, but also to some magnetic entropy due to the spontaneous magnetization collective fluctuations. We can write $\mathcal{F} = \mathcal{F}_M - \mathcal{F}_e$ for the balance of magnetic \mathcal{F}_M and electronic \mathcal{F}_e free energies participating in the processes under discussion. The observed magnetization M should result from the minimization of \mathcal{F} . We have discussed elsewhere [20] that after trivial rearrangements, the above functional \mathcal{F} can be cast into a familiar GL type form describing a second-order phase transition, namely

$$\mathcal{F}[\eta] = a\eta^2 + \frac{\beta}{2}\eta^4 - \zeta\eta^2, \quad (5)$$

where η is the order parameter, in our notations [20], the *square* of the magnetization. As usual, the equilibrium state of such a system is determined from the minimum energy condition $\partial\mathcal{F}/\partial\eta = 0$ which yields η_0 for $T < T_0$

$$\eta_0^2 = \frac{\alpha(T_0 - T) + \zeta}{\beta}. \quad (6)$$

This leads to an expression for the total magnetization

$$M = M_{av} + M_{fl}^- = M_s \left(\eta_0^2 - \frac{\zeta^2}{3\beta^2\eta_0^2} \right), \quad (7)$$

in terms of the ζ , β , and η_0 parameter of the GL free energy functional. Given the above definitions, the critical temperatures are related to each other as follows

$$T_{MI} = \left(1 - \frac{2M_0H_0}{n_e E_k(0,0) - n_i JS}\right) T_C, \quad (8)$$

with

$$T_C = \left(1 + \frac{yn_i JS}{n_e E_k(0,0)}\right) T^*, \quad y = 1 - \frac{1}{\sqrt{3}}. \quad (9)$$

where $T^* = 170K$, the peak of the GMR which "normalizes" the temperature scale in such a theory. In the above equations, $E_k(0,0) = \hbar^2/2m\xi^2(0,0)$, where $\xi(T,H)$ is the field-dependent charge carrier localization length, and m an effective electron mass. The balance of the exchange $n_i JS$ and localization induced magnetic $M_s H_0$ energies can also be described by the parameter $z = n_i JS/M_s H_0$; the mean-field expression for the "critical field" is $H_0 = 3k_B T_C/2S\mu_B$. Notice that we found $n_e/n_i \simeq 2/3$, where n_i and n_e stand for the number density of localized spins and conduction electrons respectively, from the competition between the electron-spin exchange JS and the induced magnetic energy $M_s H_0$ in analyzing the $R(T)$ data [19, 20]. The analysis of such data produces $T_C = 195K$, $JS = 40meV$, instead of 45 meV in [15].

However we hereby conjecture that the value of the exchange energy JS , whence the transition temperature, as in any mean field theory [41] depends on the type of bonding, thus on the $Mn-O-Mn$ bond environment, and calculate such an effect next.

A list of possible $Mn-O-Mn$ bond environments is given in Table I and Table II with their respective probability of occurrence, assuming statistical independence of the conditional probabilities, in other words no short range order. It is easily understood that due to the respective concentrations of La , Ca , and Y a few types of $Mn-O-Mn$ bond environments are practically relevant, each one being characterized by its "cluster critical temperature" related to the "cluster DE-effective exchange integral", see Eq.(9). Notice that due to the incommensurability of the ion content with respect to the available crystallographic site numbers, such "clusters" are unavoidable, and subsist even after repeated annealing, as later checked from the X-Ray spectrum.

The plausible explanation for an intrinsic material origin of the substructures observed in $\rho(T)$, rather than an extrinsic one as in [43], is provided by the model of Attfield et al. [44]. It is hereby used in order to evaluate whether there exist such "environmental effects" on the local distortions of the $Mn-O-Mn$ bond, thereby significantly affecting the local exchange integrals, whence the "average transition temperature(s)". Local distortions leading to specific exchange integrals responsible for magnetic transitions in (so called clusters) have been parameterised here using two quantities : (i) the *coherent* strain parameter $((r_A)^0 - \langle r_A \rangle)^2$, derived from the expression of the tolerance factor describes the deviation from the mean cation size; $(r_A)^0$ is the ideal perovskite A cation ionic radius, i.e. 1.30 Å for $LaMnO_3$ perovskites [45] and $\langle r_A \rangle$ is the mean radius of the occurring A-site cations; (ii) the statistical

variance σ^2 in the distributions of ionic radii for each local configuration; the variance measures the *incoherent* strain, i.e. the effect of disorder due to the disparity or mismatch of individual A cation radii. Thereby we indicate that different samples with the *same* doping level and tolerance factors can have quite *different* transition temperatures.

Among the clusters, we should disregard at once that formed by 4 La 's, indicated by a †) in Table 1, since this would correspond to a $LaMnO_3$ compound which is *not* ferromagnetic [46]. Only the four other main local configurations, i.e. according to the above statistical analysis (Table I) they occur more than 8% of the time, have thus been taken into account, considering specific cationic site distributions around each oxygen ion (see Fig. 4): each one is octahedrally coordinated by two Mn cations and by four A cations in the plane perpendicular to the *quasi* linear $Mn-O-Mn$ bridge. In such a first order (and reasonable) approximation the change in the spin-spin DE-integral, whence T_C , is essentially attributed to local strains resulting from oxygen atom displacements. A plot of T_C vs. $\sigma^2 + ((r_A)^0 - \langle r_A \rangle)^2$ from data calculated and reported in Table I is shown in Fig.5. This indicates a marked inverse square root relationship (Fig.5), (in contrast to Attfield estimated linear relationship [45], - markedly unphysical) allowing to rank and confirm the role of each environment on the respective transition temperatures. E.g. the 3 La ,1 Ca cluster corresponds to the GMR compound $La_{0.75}Ca_{0.25}MnO_3$ which has a transition temperature near 225K.

Further *ab initio* calculations, outside the scope of this paper, would be useful in order to estimate more exactly, the relative exchange energies for the clusters drawn in Fig.4. This would lead to establish the values the $Mn-O$ bond lengths and $Mn-O$ bond angles in the MnO_6 octahedra as a function of the environment. It is also known that the electronic band width W depends on the $Mn-O$ tilt angles [47]. These depend on the $B-O-B$ bond angles and $B-O$ lengths through the overlap integrals between the 3d orbitals of the B ion and the 2p orbitals of the O anion. Moreover W controls the critical temperature through

$$T_C \simeq W \exp(-\gamma E_{JT}) / \hbar w \quad (10)$$

where w is an appropriate optical mode frequency, and E_{JT} the Jahn-Teller (JT) energy (ca. 0.3 eV) [48, 49]. W should decrease with increasing temperature [49], leading to electronic localization at high temperature. This confirms that the discussed magnetic transitions should occur below the main M-I one indeed.

For completeness, let us point out that as in several reports one might also attempt to discuss features in terms of JT effects rather than through a DE formalism. The JT scheme considers the $Mn-O-Mn$ bond geometry *per se*, we emphasize the role of the bond environment. Both might be highly related of course.

In the same line of thought, the specific heat regimes below T_C and T_{MI} are thus easily understood from basic solid state physics as recalled here above. We

emphasize the remarkable agreement between the temperature of the anomalies in C and $d\rho/dT$ thereby illustrating the Fisher-Langer formula, i.e. $C \sim d\rho/dT$ at second order phase transitions [37].

For completeness again, let us recall that Castro et al. [24] attribute three widely spaced anomaly in the specific heat of $La_{0.875}Ca_{0.125}MnO_3$ (in order of decreasing temperature) (310 K) to the formation of magnetic polaron, (146 K) a paramagnetic to ferromagnetic transition, (80 K) a charge ordering or spin-glass transition, and the 35 K to a movement of domain walls or spin reorientation transition.

One point might still be in doubt, i.e. whether the linear T regime is a truly electronic effect or a *smooth* crossover. As an argument of a physical effect, we may argue that one should distinguish between a *smooth* and a *sharp* crossover, the latter indicating a specific energy, here a temperature or a measure of the corresponding effective exchange integral, while the former points out to disorder or inhomogeneities. In view of the well defined positions of the 94 and 156 K temperatures we might rightly consider *them* as crossovers. Keeping coherent with the above analysis we consider therefore that the temperature interval between these temperatures is the siege of a specific set of phenomena without any disorder-like effects. It might be also argued against our interpretation that the *low temperature electronic regime* giving a linear variation in temperature extends a little bit high (euphemism !) in temperature. This would be valid but only if disregarding the marked importance of the electronic effects in such materials for which the M-I phase transition occurs at rather *high* temperature in fact.

Thus we seem to have accounted for the observed temperature dependences of the specific heat in $La_{0.6}Y_{0.1}Ca_{0.3}MnO_3$, in terms of ideas derived from the DE localization model for GMR materials. All such features are in agreement with the usual microscopic spin-polaron and electronic localization theories. Next, concerning the power law exponent less than unity here above observed in the specific heat temperature behavior the matter is not so trivial. A $C \simeq T^{2/3}$ law as found at high temperature can be discussed in terms of the fractal dimension of the conducting network in the so-called insulating phase, as in Orbach description of random media excitations [50]. It is known that depending on the excitation spectrum, be it of bosons(b), i.e. phonons and magnons, or fermions(f), i.e. electrons, their density of states depends on the effective dimensionality $\tilde{\delta}$ of the system, i. e.

$$\mathcal{D}(\omega) \sim \omega^{(\tilde{\delta}_b-1)} \quad (11)$$

or

$$\mathcal{D}(\epsilon) \sim \epsilon^{(\tilde{\delta}_f/2)-1} \quad (12)$$

for bosons and electrons respectively, thus giving respectively a specific heat behavior like

$$C_\omega \sim T^{\tilde{\delta}_b} \quad (13)$$

and

$$C_\epsilon \sim T^{(\tilde{\delta}_f - 1)/2} \quad (14)$$

for the phonon and electron contributions in a truly three dimensional system. Therefore the exponent $2/3$ can be the signature of a percolation network for the hopping charge carriers with a (very reasonable) effective dimensionality $\tilde{\delta} = 7/3$ in the less conducting (high temperature) regime. This is easily contrasted to the linear regime in the (low temperature) conducting phase, and the appearance of an electronic transition at intermediate temperatures.

4 Conclusion

On one hand, we have observed on a log-log plot three regimes for the specific heat in a temperature range encompassing the charge carrier localization temperature T_{MI} and the magnetic transition temperature T_C . At not too low temperature, a collective spin excitation or magnon signature ($C \simeq T^{3/2}$) is found as for what we could thus call a magnon-polaron regime or magneto-polaron excitations in such manganites. A simple T law occurs before the transitions. A $C \simeq T^{2/3}$ law is found at high temperature and is interpreted in terms of the fractal dimension of the conducting (hopping) network in the so-called insulating phase.

On the other hand, in the temperature regime near the drastic magnetic and charge localization transitions, the report well illustrates the Fisher-Langer formula, i.e. $C \sim d\rho/dT$ at second order phase transitions [37]. The various $Mn - O - Mn$ bond environments, within the model of Attfield [45], explain the complex features of the transition region, though we disagree with Attfield on the analytical form of the relationship between the transition temperatures and the strains.

In so doing the temperature dependence of the regimes in the specific heat (and the electrical resistivity) can be well accounted for as due to electrons *and* so called spin-polarons *and* magnon-polarons. Thereby we emphasize the role of *collective* excitations beyond the mere *localized* spin (scattering) background. During the final writing of this paper, we noticed one by Huhtinen et al. [22] which explains the overall behavior of $\rho(T)$ as a weighted sum of a variable range hopping mechanism and of itinerant electrons. In the latter, they use a $T^{4/5}$ electron-magnon interaction term as well in the $\rho(T)$ fit.

The results are supported by a free energy functional of Ginzburg-Landau (GL) type describing magnetic phase transitions near such temperatures. We pin point the possible occurrence of separated and competing phase transitions

depending on the A and R ion distribution near the $Mn-O-Mn$ bond responsible for the GMR effect. This leads to a formal description of the specific heat as an equilibrium property. The case of the electrical resistivity temperature derivative can next be understood within this framework, as due to electron "critical scattering processes" of correlated (localized) spin fluctuations. Notice that we do not discuss here whether the conduction mechanism differs above and below T_C , as attempted elsewhere in order to explain optical spectra in related materials, i.e. $La_{0.67-x}Y_xBa_{0.33}MnO_3$ [51]. Moreover those different magnetic cluster scattering processes are weakly relevant for the overall resistance behavior which has a metallic character up to the localization transition.

It is interesting to re-emphasize that we associate each critical temperature, with an exchange integral for a specific *finite* size cluster, one critical temperature usually characterizing a *cooperative* phenomenon. This is an amazing demonstration of so many observed long range cooperative phenomena due to short range interactions; see for example a calculation of a diverging susceptibility for short range spin-spin interactions in [41]. Moreover, the cooperativeness is still manifested in the fact that only the clusters having a concentration larger or as large as the order of magnitude of the percolation concentration give a remarkable effect. After this paper was reviewed we came across an interesting study of critical exponents at CMR transitions [52] where the above comment is outlined. We quote a few lines : "The DE interaction has a distinguishable property compared to ordinary exchange interactions in spin systems. Effective ferromagnetic interaction is induced by the kinetics of electrons which favor extended states with ferromagnetic spin background to gain the kinetic energy. If we integrate out the electron degrees of freedom to describe the action as a function of spin configurations, it is necessary to introduce effective long-range two-spin interactions as well as multiple-spin interactions which depend on sizes and shapes of (the) ferromagnetic domain structure. The range of the interaction is determined (in order) to minimize the total free energy for charge and spin degrees of freedom. As the system approaches the critical point, the magnetic domain structure fluctuates strongly. Thus, it is highly nontrivial how the DE interaction is renormalized, whether it is renormalized to a short-range one, or (how) the long-range and the multiple-spin interactions become relevant to cause the mean-field-like transition through suppression of fluctuations. The results ... indicate that the universality class of the ferromagnetic transition in the DE model is consistent with that of models with short-range interactions."

As we mentioned in the introductory part, along with lowering the Curie point, Y substitution brings about other important effects indeed. Namely, it drives the magnetic structure closer to a canted AFM phase (which occurs [2] at $T_{AFM} \ll T_C$) thus triggering the development of local AFM fluctuations within the parent FM matrix. In turn, these fluctuations cause a trapping of spin polarized carriers in a locally FM environment leading to hopping dominated transport of charge carriers between thus formed magneto-polarons, for the

whole temperature interval. In the low temperature conducting ferromagnetic phase, the collective magnon signature has not to be neglected neither on ρ nor C .

It is worth noting that the here above experimental and theoretical results corroborate magneto-transport measurements and subsequent analysis on the temperature behavior of the MTEP [20] in terms of *strong magnetic fluctuation effects* near the critical temperature(s).

Acknowledgments

Part of this work has been financially supported by the Action de Recherche Concertées (ARC) 94-99/174. MA and AG thank CGRI for financial support through the TOURNESOL program. MA and LH thank S. Sergeenkov for discussions and the University of Liège Research Council for an equipment grant. We thank J. C. Grenet and R. Cauro, Laboratoire de Thermodynamique Expérimentale, Université de Nice-Sophia Antipolis, Parc Valrose F-06000 Nice, Cedex 02, France for providing the samples. Thanks to K. Ivanova for helping us in the submission process.

Table 1: Statistical table of the percentage of the most often expected ($> 8.0\%$) [La,Y,Ca]-clusters in the ABO_3 structure for one $La_{0.6}Y_{0.1}Ca_{0.3}MnO_3$; notations as in Fig.4. A cluster is considered to be made of four cations placed on the corners of a square itself in a perpendicular plane to the quasi linear $Mn - O - Mn$ bond. The clusters are ranked according to their most probable joint frequency of occurrence, assuming independent probabilities. The displayed frequency does not take into account a possible short range order for the (*) clusters for which several ion configurations are possible. The third column gives the sum of the coherent and incoherent strain parameter $\sigma^2 + ((r_A)^0 - \langle r_A \rangle)^2$. The corresponding critical temperature is indicated

	Cluster type	frequency	total strain	critical temperature
I	$3La, 1Ca$	25.92	0.009	146
II	$2Ca, 2La(*)$	19.44	0.011	130
-	$4La(\dagger)$	12.96	-	-
III	$2La, 1Ca, 1Y$	12.96	0.018	108
IV	$3La, 1Y$	8.64	0.020	94

Table 2: Statistical table of the percentage of more rarely expected [La,Y,Ca]-clusters in the ABO_3 structure for $La_{0.6}Y_{0.1}Ca_{0.3}MnO_3$ with notations as in Table I

Cluster type	frequency	Cluster type	frequency
$3Ca, 1La$	6.48	$2Ca, 1La, 1Y$	6.48
$2La, 2Y(*)$	2.16	$1La, 1Ca, 2Y$	2.16
$3Ca, 1Y$	1.08	$4Ca(\dagger)$	0.81
$2Ca, 2Y(*)$	0.54	$1La, 3Y$	0.24
$1Ca, 3Y$	0.12	$4Y(\dagger)$	0.01

References

- [1] For a detailed discussion and extensive references, see *Colossal Magnetoresistance, Charge Ordering and Related Properties of Manganese Oxides*, edited by C. N. R. Rao and B. Raveau (World Scientific, Singapore, 1988); J. M. D. Coey, M. Viret, and S. Von Molnar, *Adv. Phys.*, **48**, 167 (1999).
- [2] A.P. Ramirez, *J. Phys. Condens. Matter* **9**, 8171 (1997).
- [3] S. Jin, H.M. O'Bryan, T.H. Tiefel, M. McCormack, and W.W. Rhodes *Appl. Phys. Lett.* **66**, 382 (1995)
- [4] H.L. Ju, C. Kwon, Qi Li, R.L. Greene, and T. Venkatesan, *Appl. Phys. Lett.* **65**, 2108 (1994).
- [5] P. Schiffer, A.P. Ramirez, W. Bao, and S.-W. Cheong, *Phys. Rev. Lett.* **75**, 3336 (1995).
- [6] P.G. Radaelli, D.E. Cox, M. Marezio, S.-W. Cheong, P. Schiffer, and A.P. Ramirez, *Phys. Rev. Lett.* **74**, 4488 (1995).
- [7] J. Barrat, M.R. Lees, G. Balakrishnan, and D. McPaul, *Appl. Phys. Lett.* **68**, 424 (1996).
- [8] J. Fontcuberta, M. Martinez, A. Seffar, S. Pinol, J.L. Garcia-Munoz, and X. Obradors, *Phys. Rev. Lett.* **76**, 1122 (1996).
- [9] J.L. Garcia-Munoz, M. Suaaidi, J. Fontcuberta, and J. Rodriguez-Carvajal, *Phys. Rev. B* **55**, 34 (1997).
- [10] J. Fontcuberta, V. Laukhin, and X. Obradors, *Appl. Phys. Lett.* **72**, 2607 (1998).

- [11] J. Fontcuberta, Ll. Balcells, B. Martinez, and X. Obradors, in *Nanocrystalline and Thin Film Magnetic Oxides* I. Nedkov and M. Ausloos, Eds., NATO ASI Series vol. 72 (Kluwer, Dordrecht, 1999) pp. 105-118.
- [12] Qi Li and H.S. Wang, in *Nanocrystalline and Thin Film Magnetic Oxides*, I. Nedkov and M. Ausloos, Eds., NATO ASI Series vol. 72 (Kluwer, Dordrecht, 1999) pp. 133-144.
- [13] A.J. Millis, P.B. Littlewood, and B.I. Shraiman, Phys. Rev. Lett. **74**, 5144 (1995); *ibid* **77**, 175 (1996).
- [14] H. Roder, J. Zang, and A.R. Bishop, Phys. Rev. Lett. **76**, 1356 (1996).
- [15] W.E. Pickett and D.J. Singh, Phys. Rev. B **53**, 1146 (1996).
- [16] L. Sheng, D.Y. Xing, D.N. Sheng, and C.S. Ting, Phys. Rev. Lett. **79**, 1710 (1997).
- [17] C.M. Varma, Phys. Rev. B **54**, 7328 (1996).
- [18] Z.B. Guo, Y.W. Du, J.S. Zhu, H. Huang, W.P. Ding, and D. Feng, Phys. Rev. Lett. **78**, 1142 (1997).
- [19] S. Sergeenkov, H. Bougrine, M. Ausloos, and A. Gilabert, JETP Lett. **70**, 141 (1999)
- [20] S. Sergeenkov, H. Bougrine, M. Ausloos, and A. Gilabert, Phys. Rev. B **60**, 12 322 (1999)
- [21] N. Vandewalle, M. Ausloos, and R. Cloots, Phys. Rev. B **59**, 11909 (1999)
- [22] H. Huhtinen, R. Laiho, K. G. Lisunov, V. N. Stamov and V. S. Zakhvalinskii, J. Magn. Magn. Mater. **238**, 160 (2002)
- [23] B. Vertruyen, R. Cloots, A. Rulmont, G. Dhalenne, M. Ausloos, and Ph. Vanderbemden, J. Appl. Phys. **90**, 5692 (2001)
- [24] M. Castro, R. Burriel, and S.W. Cheong, J. Magn. Magn. Mater. **196-197**, 512 (1999)
- [25] T. Okuda, Y. Tomioka, A. Asamitsu, Y. Tokura, Phys. Rev. B **61**, 8009 (2000)
- [26] J. E. Gordon, C. Marcenat, J. P. Franck, I. Isaac, Guanwen Zhang, R. Lortz, C. Meingast, F. Bouquet, R. A. Fisher, and N. E. Phillips, Phys. Rev. B **65**, 024441 (2001)
- [27] A.L. Cornelius, B. Light, J.J. Neumeier, <http://arXiv.org/abs/cond-mat/0108239>

- [28] N. F. Mott, Proc. Roy. Soc. A **153**, 699 (1936); ibid. **156**, 368 (1936)
- [29] T. Van Peski-Timbergen and A.J. Dekker, Physica **29**, 917 (1963).
- [30] P.G. De Gennes and J. Friedel, J. Phys. Chem. Solids **4**, 71 (1958).
- [31] T. Kasuya, Rep. Prog. Phys. **16**, 58 (1956); ibid. **22**, 227 (1959).
- [32] M. Ausloos and K. Durczewski, Phys. Rev. B **22**, 2439 (1980).
- [33] M. Ausloos, in *Magnetic Phase Transitions*, M.Ausloos and R.J. Elliott, Eds. (Springer Verlag, Berlin-Heidelberg, 1983) pp. 99-129.
- [34] S. Dorbolo, M. Ausloos and M. Houssa, Phys. Rev. B **57**, 5401 (1998).
- [35] J.B. Sousa, M.M. Amado, R.P. Pinto, J.M. Moreira, M.E. Braga, M. Ausloos, J.P. Leburton, J.C. Van Hay, P. Clippe, J.P. Vigneron, and P. Morin, J. Phys. F **10**, 933 (1980).
- [36] M. Ausloos and Ch. Laurent, Phys. Rev. B **37**, 611 (1988).
- [37] M.E. Fisher and J.S. Langer, Phys. Rev. Lett. **20**, 665 (1968).
- [38] D.J.W. Geldart and T.G. Richard, Phys. Rev. B **12**, 5175 (1975).
- [39] D.J.W. Geldart, Phys. Rev. B **15**, 3455 (1977).
- [40] Ch. Kittel and C. Y. Fong, *Quantum Theory of Solids*, Wiley, New York, 1987.
- [41] H.E. Stanley, *Introduction to Phase Transitions and Critical Phenomena*, Clarendon Press, Oxford, 1968.
- [42] P. Wagner, I. Gordon, L. Trappeniers, J. Vanacken, F. Herlach, V.V. Moshchalkov, and Y. Bruynseraede, Phys. Rev. Lett. **81**, 3980 (1998).
- [43] M. Ausloos, J.P. Leburton and P. Clippe, Solid State Commun. **33**, 75 (1980)
- [44] L. M. Rodriguez-Martinez and J. P. Attfield, Phys. Rev. B **54**, R15622 (1996)
- [45] J. P. Attfield, Int. J. Inorg. Mater. **3**, 1147 (2001)
- [46] J.L. Garcia-Munoz, J. Fontcuberta, M. Suaaidi, and X. Obradors, J. Phys. Condens. Matter **8**, L787 (1996).
- [47] M. Melarde, J. Mesot, P. Lacorre, S. Rozenkranz, P. Fischer, and K. Gobrecht, Phys. Rev. B **52**, 9248 (1995)
- [48] G. Zhao, K. Conder, H. Keller, and K.A. Muller, Nature **381**, 676 (1996)

- [49] L. Wang and X. Zhang, Physica C **371**, 330 (2002)
- [50] T. Nakayama, K. Yakubo and R. L. Orbach, Rev. Mod. Phys. **66**, 342 (1994)
- [51] N.G. Bebenin, N.N. Loshkareva, Yu. P. Sukhorukov, A.P. Nossov, R.I. Zainullina, V.G. Vassiliev, B.V. Slobodin, K.M. Demchuk, and V.V. Ustinov, Solid State Commun. **106**, 357 (1998)
- [52] N.Furukawa and Y. Motome, arxiv:cond-mat/0107172; to be published in Appl. Phys. A **75**, xxx (2002)

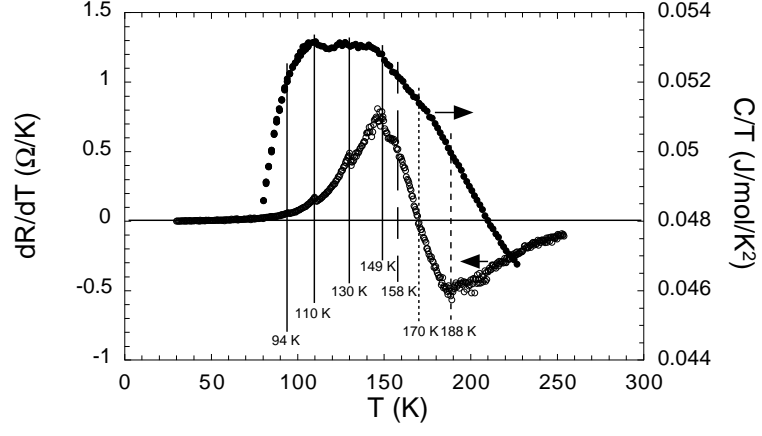


Figure 1: Temperature behavior of the temperature derivative of the electrical resistivity, i.e. $d\rho(T)/dT$ and the value of C/T where C is the specific heat of $La_{0.6}Y_{0.1}Ca_{0.3}MnO_3$

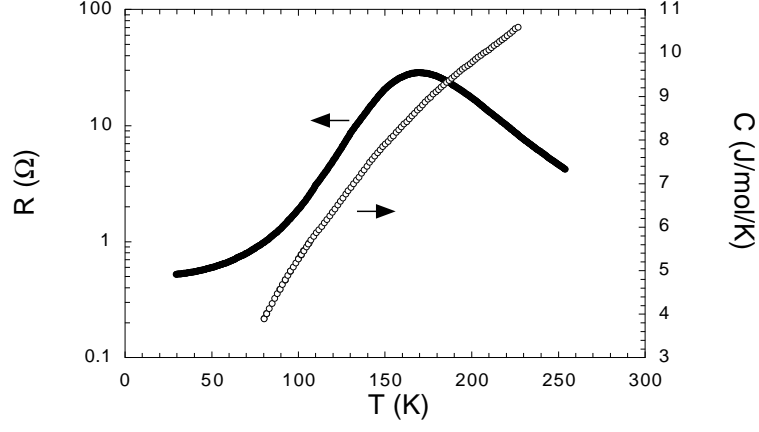


Figure 2: Temperature behavior of the specific heat C and the resistivity ρ at $B = 0$ for $La_{0.6}Y_{0.1}Ca_{0.3}MnO_3$

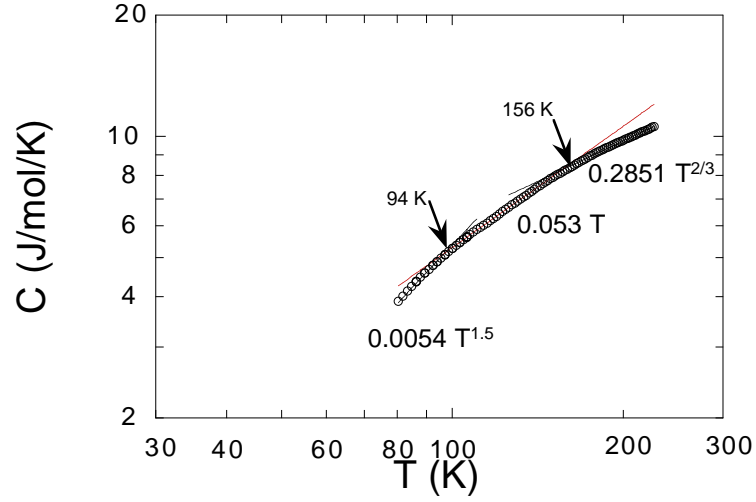


Figure 3: Temperature behavior of the specific heat of $La_{0.6}Y_{0.1}Ca_{0.3}MnO_3$ on a log-log plot. The best fits to the data points lead to the indicated slopes

Figure 4: Sketch of the four main relevant clusters of $Mn - O - Mn$ bonds in presence of La , Ca , and Y at A sites in the ABO_3 structure.

Figure 5: Plot of T_C vs. the total coherent and incoherent strain parameter $\sigma^2 + ((r_A)^0 - \langle r_A \rangle)^2$ from data collected in [45] for the main relevant clusters of $Mn - O - Mn$ bonds in presence of La , Ca , and Y distributed on A sites in the ABO_3 structure